Earth Surface Processes and Landforms
Earth Surf. Process. Landforms, **23**, 1171–1183 (1998)

DESIGN AND FIELD TEST OF A CONTINUOUSLY WEIGHING, TIPPING-BUCKET ASSEMBLY FOR AEOLIAN SAND TRAPS

BERNARD O. BAUER* AND STEVEN L. NAMIKAS

Department of Geography, University of Southern California, Los Angeles, California 90089-0255, USA

Received 26 June 1997; Revised 21 September 1997; Accepted 16 January 1998

ABSTRACT

A new tipping-bucket assembly (T-BASS) for aeolian sand traps has been designed and field tested with encouraging results. It facilitates high-frequency monitoring of sediment flux over extensive time periods, and therefore offers improved performance over other continuously weighing mechanisms that are generally limited to either a small total-load capacity or poor resolving ability. The T-BASS is a modified version of the tipping-bucket meteorological rain gauge mounted on a cantilever and pulley system linked to an electronic load cell. As trapped sand accumulates in one of the buckets, the increasing mass exerts a downward force on the cantilever arm, which translates into a slight deflection of the thin-beam element of the load cell. The resulting voltage output is proportional to the load, and the analogue signal may be monitored by a data-acquisition system. Eventually the bucket fills to capacity and tips, the sediment load is emptied into a reservoir container, the other bucket of the bucket pair is positioned beneath the funnel, and the system is automatically reset to zero load for continued measurement. In this way, a high-frequency record of sediment accumulation is obtained.

Field testing of five prototypes demonstrated that the T-BASS can be configured to yield: (i) linear calibrations (for conversion of voltage to gram weight) with R^2 values exceeding 0·99; (ii) weight resolution of 0·1 g or better depending on load-cell specifications and bucket capacity; and (iii) detailed temporal information (order of 1 s) on sediment flux allowing investigation of its relation to attributes of the wind field. Suggested modifications may produce improved performance in future versions. © 1998 John Wiley & Sons, Ltd.

KEY WORDS: aeolian transport; sediment trap; high-frequency measurement

INTRODUCTION

Scientific understanding of aeolian sedimentary processes has advanced considerably since the seminal works of Bagnold (1936, 1941). These insights have accrued as a result of extensive efforts in the field and laboratory, and through theoretical and numerical modelling studies. Indeed, the latter have advanced to a degree that further development in some areas has been constrained by our inability to collect reliable field data to test critical modelling assumptions and to verify or refute their implications for aeolian transport mechanics (Anderson *et al*., 1991; Butterfield, 1993). Although considerable attention has been devoted to attributes of the wind field, particularly within the domain of boundary-layer meteorology and agricultural physics, relatively few field measurements of sediment flux over deformable sand surfaces exist at the spatial and temporal resolution needed to address such fundamental issues as the integrity of the widely assumed cubic power relation between shear velocity and sediment-transport rate, the existence of an easily defined, discrete threshold shear velocity for sediments of a specified size range, the tendency towards an equilibrium (saturation) transport rate for a given shear velocity, or the role of the saltation layer as an aerodynamic roughness-enhancing element. Although the dominant concern has always been with sediment transport *per se*, one of the weakest links constraining our ability to advance our conceptual understanding of aeolian transport mechanics remains the questionable accuracy, limited precision and crude temporal resolution of sediment-flux measurements obtained in the field.

* Correspondence to: B. O. Bauer, National Science Foundation (Geography and Regional Science Program), 4201 Wilson Boulevard, Arlington, Virginia 22230, USA
E-mail: bbauer@nsf.gov
Contract/grant sponsor: Geography and Regional Science Program (National Science Foundation)
Contract/grant numbers: SES-9158230; SES-9511529

CCC 0197-9337/98/131171–13 $17.50

Four basic approaches to field measurement of aeolian sediment flux are recognized (Sherman, 1990): they involve vertical traps, horizontal traps, topographic traps and sediment tracers. A time-integrating technique is most frequently employed, in which traps are deployed to collect sediment for periods of several minutes (e.g. Arens, 1994; Nordstrom *et al*., 1996; Gares *et al*., 1996), hours (e.g. Greeley *et al*., 1996), days (e.g. Horikawa *et al*., 1984) or longer (e.g. Fryberger *et al*., 1984; Goldsmith *et al*., 1990; Kroon and Hoekstra, 1990; Davidson-Arnott and Law, 1996). The total weight of accumulated sediment in the trap (or estimated from topographic change) is used to calculate a mean sediment transport rate averaged over the entire period of trap deployment. This approach provides only crude information in the time domain, and therefore relatively little is known about the unsteady and non-uniform character of aeolian saltation systems (Fryberger *et al*., 1979; Butterfield, 1991; Bauer *et al*., 1996).

A small number of field studies have attempted to redress these empirical shortcomings by implementing some form of continuously weighing sand trap using either force transducers (e.g. Fryberger *et al*., 1979; Lee, 1984, 1987; Butterfield, 1991; Jackson, 1996; Nickling and Davidson-Arnott, pers. comm.) or sonic devices such as the 'saltiphone' (e.g. Spaan and van den Abeele, 1991; van Dijk and Hollemans, 1991; Arens, 1996) to improve the temporal resolution of sediment-flux measurements. Almost universally, these efforts have experienced non-trivial technological impediments. The saltiphone, for example, is a grain-impact counting device (mass fluxes are not recorded directly) that is difficult to calibrate for field deployment because of the many extraneous sources of noise. The utility of electronic force transducers, on the other hand, is limited by performance constraints of the load cell or electronic balance, in particular the ratio of specified accuracy and precision to load capacity. Only the most technically advanced (hence most expensive) load cells or balances offer milligram precision (i.e. tens to hundreds of sand grains) in combination with a maximum load capacity exceeding 1 kg (i.e. more than about 5–10 min of intense transport depending on trap opening width). Butterfield (1993) points out that mass-flux time series need to be measured at frequencies of about 1 Hz or faster for development of realistic sand transport relations; that is, the measuring mechanism in the trap also needs to be of a fast-response type. It must be sensitive enough to respond to small changes in the transport rate from second to second, yet of sufficient capacity to allow for long-term (tens of minutes to hours) data collection. Further, the spatial variability inherent to natural transport systems (e.g. Bauer *et al*., 1996) argues strongly in favour of inexpensive devices that facilitate deployment of spatial arrays. In order to acquire field data that satisfy the stringent high-frequency requirements of the numerical models and are also of sufficient duration to characterize the long-term unsteadiness in natural wind events, it will become necessary to surmount the limitations of extant trap designs.

This paper describes a new tipping-bucket assembly (T-BASS) that facilitates high-frequency measurement of aeolian sediment flux for unlimited time periods. The design is based on the tipping-bucket mechanism incorporated into the well known meteorological rain gauge of the same name. An inexpensive load cell is incorporated into the assembly to sense the weight of sand accumulating in either collection bucket as it fills. The buckets are designed to tip at a prescribed weight approaching the maximum capacity of the load cell. A voltage time series is produced consisting of smoothly increasing curve segments interrupted by short-term, bucket-tip events that reset the system to its starting state. In this way, a very detailed record of sediment flux can be collected over a lengthy wind-storm event without stopping the data-collection run to empty and reinstall the trap. In the following sections, we will: (1) describe the design and principle of operation of the tipping-bucket assembly; (2) discuss the set-up and calibration procedures used in this study; (3) present data from prototype traps deployed during a field experiment that demonstrate the potential of the new assembly; and (4) suggest future modification that may yield improved performance.

DESIGN AND PRINCIPLE OF OPERATION

The tipping-bucket assembly (T-BASS) is one portion of an integrated aeolian sediment trap that consists of an above-ground trapping shell and a below-ground housing box; the latter contains the T-BASS, a funnel and a reservoir container, all of which can be accessed via a top-opening entry hatch (Figure 1). The trapping shell can be of any design, including the wedge or cylindrical passive-collector styles most commonly employed in aeolian field studies (e.g. Leatherman, 1978; Shao *et al*., 1993; Gares *et al*., 1996; Greeley *et al*., 1996). In the

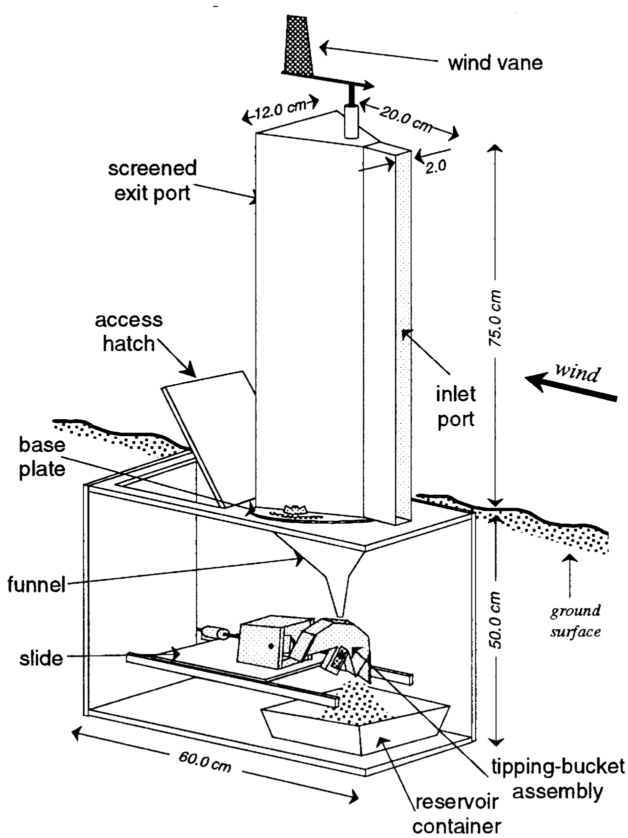

Figure 1. Schematic diagram showing assembled integrated trap with view of interior

present study we employed a new wedge-shaped design (Nickling and McKenna Neuman, 1997) that promises improved efficiency because of the addition of an inlet duct leading ino the trapping orifice which causes eddy shedding to be advected downwind of the trap opening. These shells were mounted on a wooden base plate into which were routered two symmetrical, semi-circular channels allowing the shell unit to be rotated across a horizontal swath of 60° to accommodate the mean wind direction.

The T-BASS is mounted immediately beneath a funnel that conveys trapped sediment to the tipping buckets (Figure 1). To facilitate positioning of the T-BASS, the entire assembly was bolted to an adjustable platform that slides along rails mounted to the sides of the buried housing. A plastic reservoir container serves to collect sediment as it is tipped out of the buckets. The only limitation on the total duration of trap deployment is the capacity of this container.

The T-BASS comprises three integrated components (Figure 2A): (1) the tipping-bucket mechanism; (2) a cantilever system; and (3) an electronic load-cell unit. In general, trapped sand falls through the funnel into one of the buckets of the tipping-bucket mechanism where the accumulating weight exerts a force on the cantilever arm. This force is translated, via a pulley-and-string mechanism, to the electronic load cell, which generates a corresponding DC voltage that can be monitored and recorded by any standard multimeter or data-acquisition system. The main components of the T-BASS body were milled from PVC blocks and assembled using stainless-steel bolts.

Tipping-bucket mechanism

The design of the tipping-bucket mechanism (Figure 2B) is a modified version of those incorporated into standard meteorological rain gauges. The essential differences include: (1) a smoothly curved bucket bottom with varying radius of curvature; (2) a freely moving, hinged, aluminium trap door that covers each bucket

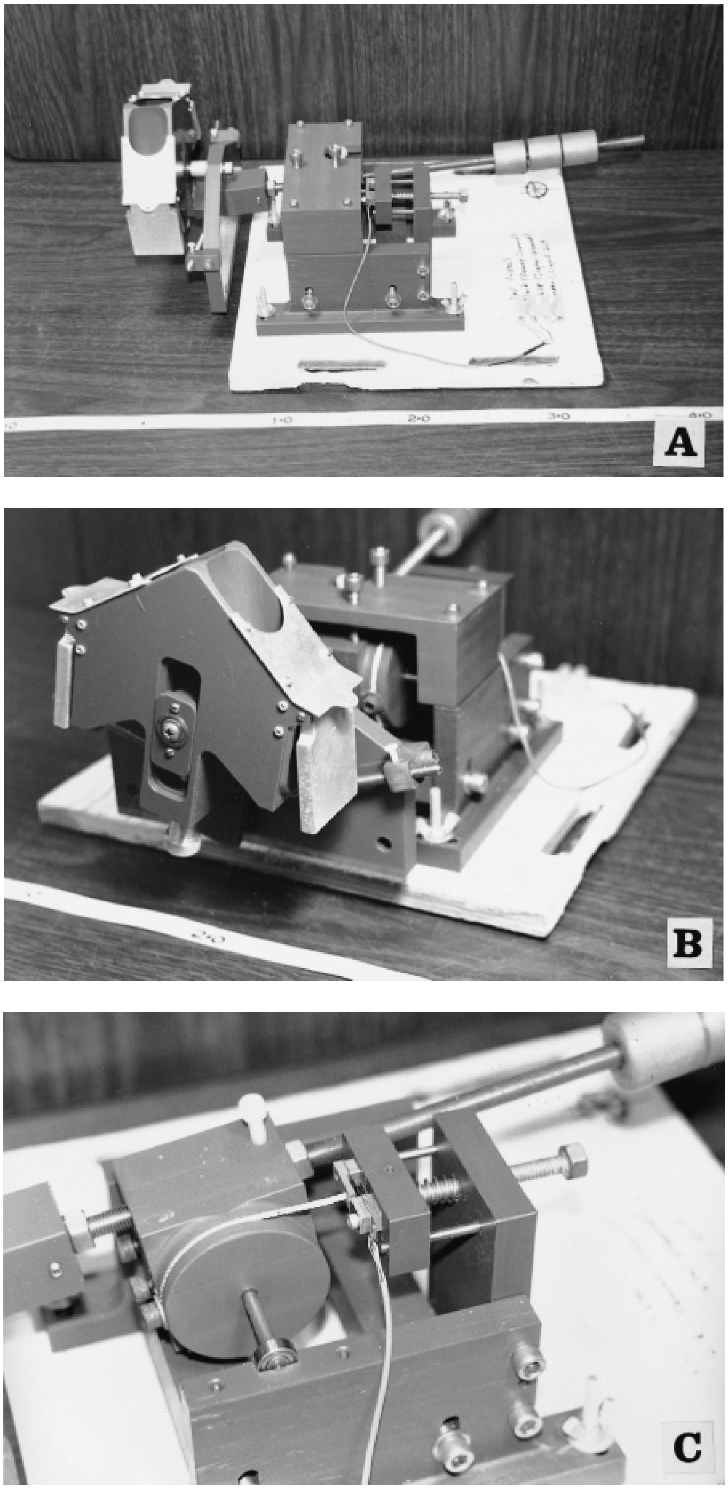

Figure 2. (A) Overall view of assembled T-BASS mounted on wooden platform. (B) Front, close-up view of tipping-bucket mechanism showing: (i) aluminium trap doors in open (right) and closed (left) positions; (ii)sediment opening on top with aluminium 'roof' on either side; (iii) adjustable, channellized pivot-axle mechanisms with small set screws in front and large, knurled turning bolt at bottom; and (iv) right-hand side stopper screw that restricts the tipping action of the bucket. (C) Oblique, side view of cantilever system with upper portion of support structure removed, showing: (i) cantilever rod and axle block; (ii) circular pulley; (iii) axle and bearings seated in the support structure; (iv) string connection between pulley and load cell; and (v) load-cell mounting platform with adjustment bolt and guide rails

opening; (3) an aluminium 'roof' on each bucket; and (4) an adjustable, channelled pivot-axle mechanism. The standard meteorological rain gauge will not work for aeolian applications because the bucket bottoms have linear facets. Sand accumulates at the apex of these facets in an angle-of-repose pile and fails to spread out laterally (as does water). As a result, the centre of gravity of the accumulating sand pile does not migrate outward away from the pivot axis, and the force imbalance that would induce a bucket tip never develops. The T-BASS buckets, on the other hand, have smoothly sloping bottoms of varying radius of curvature that direct accumulating sediment to the distal end of the bucket. In this way, the centre of gravity is shifted outward as sediment accumulates. A hinged aluminium gate at the bucket opening prevents sand from spilling out of the bucket (Figure 2B). When the bucket tips, gravity causes the gate to swing open thereby allowing the sediment load to pour out freely. The aluminium roof prevents sand grains from bouncing out of the bucket as they fall from the funnel into the bucket bottom.

The adjustable, channelled pivot-axle mechanism allows the tipping bucket to be raised or lowered relative to the pivot axis (Figure 2B). Lowering (raising) the vertical position of the tipping bucket causes the mechanism to tip at lesser (greater) weight in each bucket. There are, however, lower and upper limits to the tipping weight depending on the specific design of the tipping-bucket mechanism. It was found that for the tipping mechanism to work effectively, the centre of gravity of the unweighted system must be above the horizontal pivot plane and a slight lateral instability in the distribution of weight needs to be retained; that is, the centre of gravity needs to shift from one side of the pivot axis to the other as an empty bucket fills with sediment. Lowering the bucket too far along the channel causes the centre of gravity to shift below the pivot plane and the bucket stabilizes, holding a perfectly vertical position like a plumb bob.

Cantilever system

The cantilever system (Figure 2C) consists of a threaded rod with a mounting block for the tipping-bucket mechanism on one end and a set of adjustable brass counterweights on the other. The rod is threaded through a PVC axle block that has a circular pulley milled onto one side. The rod can be turned through the axle block to lengthen or shorten the cantilever action, allowing the force imparted to the load cell by accumulating grains to be magnified by up to a factor of about ten. This considerably extends the range of transport rates under which the device can operate. The pulley is an integral, fixed part of the axle block and therefore rotates with it as the cantilever rod moves up or down. A stainless steel axle passes through the centre of the axle block and is mounted in high-quality bearings embedded in the sides of the support structure. Two large set screws penetrate the top of the support structure and they can be adjusted to prevent or restrict the cantilever motion so as to prevent damage to the load cell during installation and operation.

The mounting block for the tipping-bucket mechanism has a 10° offset from the vertical so that the tipping bucket retains a near-vertical position as the cantilever rod tilts downward (Figure 2A). Through trial and error, it was found that such an initial 'dip' to the cantilever rod helped to linearize the force translation from the bucket to the load cell. The mounting block also has stopper screws mounted on either side that constrain the back and forth swing of the tipping bucket. The range of this swing, and hence the position of these stopper screws, is critical to the tipping action of the bucket (i.e. how much sediment is needed to initiate a tip) because a greater range of swing implies that the centre of gravity of the unweighted system is positioned correspondingly farther from the pivot axis. Therefore it takes greater sediment mass in the bucket to shift the centre of gravity of the weighted system to the other side of the pivot axis before a tip can be initiated.

Electronic load-cell unit

The load cell used in the prototype is a thin-beam device with a rated operational load capacity of 113 g, equivalent to about 2–3 mm of linear deflection (OMEGA Model LCL-113g). Voltage output is 2 mV/V with an excitation requirement of 5–10 VDC (12 VDC max.), a safe overload rating of 150 per cent FS, a combined error of 0·25 per cent FS, and a temperature-compensated operating range between –5 and 50°C. The load cell is mounted on a vertical platform so that its centre is aligned with the horizontal tangent of the upper pulley arc (Figure 2C). An adjustable bolt controls the distance from the load cell to the pulley, and the string that connects the pulley to the load cell is pulled taut by backing off the platform. Any subsequent downward force on the

tipping bucket (due to accumulating sand grains) induces a torque that is translated through the pulley and string to the load cell.

SET-UP AND CALIBRATION PROCEDURES

Considerable flexibility was designed into the prototype T-BASS because of uncertainty in knowing at the outset whether a permanently configured assembly with no adjustable components could be made to perform as desired. Each unit was adjusted to yield a tipping weight of about 8–10 g with a force magnification to the load cell of about 10 times (i.e. 80–100 g). The counterweights were adjusted to compensate for the empty weight of the tipping-bucket mechanism while maintaining a slightly positive stress on the load cell (about 10–20 per cent of full scale). This produced a nearly linear force translation through the mechanical linkages and a nearly linear voltage output from the load cell corresponding to the middle 70–80 per cent of its range. In theory, this configuration should have yielded a resolution of about 25 mg (approximately the weight of about 200 cubic grains of quartz sand with a diameter of 0·38 mm). In practice, the mechanical linkages in the T-BASS introduce additional measurement uncertainty (e.g. bearing friction, string elasticity) so that the resolving capability of the entire assembly was estimated to be of the order of 100 mg or less. It should be noted that the exact resolution can be adjusted upward or downward depending on how the force magnification of the cantilever-and-pulley system is configured. However, it may not always be desirable to strive for greater resolution. As resolution is enhanced, the full-scale range of the load cell is decreased and the bucket-tip frequency for any given transport rate increases. Further, a more sensitive system is likely to be susceptible to wind-loading effects within the trap cavities, generating noise in the measured signal that is difficult to compensate for (cf Butterfield, 1991, 1993).

Given the many adjustable mechanical linkages in these prototype units and the many potential sources of signal degradation between the load-cell voltage output and the data-acquisition system (varying cable resistance, poor power source, dirty electrical contacts, atmospheric moisture), it was deemed most appropriate to calibrate the T-BASS units after installation in the field, rather than beforehand in the laboratory. The housing boxes were buried flush with the sand surface and the T-BASS platforms were installed and levelled. Dozens of small, hexagonal nuts of similar known weight (1·13 g) were then tossed individually into the funnels of the installed traps. The output voltages were recorded by the data-acquisition system at a sampling rate of 5 Hz. After every toss, several seconds were allowed to pass so that the T-BASS could stabilize and produce a constant voltage output at that accumulated weight. Eventually the bucket mechanism tipped, the T-BASS reset itself to its unweighted state, and the procedure was repeated. Figure 3 shows the calibration runs from two of the five T-BASS traps deployed during the field experiment. Note the spiky oscillations evident in the upper trace (T-BASS no. 1). These are due to the ‘jolt’ that the system receives when a hexagonal nut (representing about 10–15 per cent of the full load) falls from the funnel into the bucket. The oscillations are short-lived (less than 1–2 s), and their damping rate and magnitude differ from one unit to the next depending on detailed adjustment of the various components. Such spikes and oscillations did not occur when sand was poured continuously into the funnel.

The digital voltage records obtained from these calibration runs were analysed to yield a series of voltage-versus-weight pairings for each of the five T-BASS traps installed in the field. Since the units were not configured to exact specifications, their tipping weights differed slightly (between 8 and 10 g or six and eight hexagonal nuts). Once set, however, any one bucket tips at the same weight every time. Table I gives an example of such voltage-versus-weight pairings, and the regression coefficients demonstrate how repeatable the output can be when the system is set up correctly. Figure 4 shows the regression curves obtained for the T-BASS calibration runs presented in Figure 3. In each case, there were five complete bucket fill-and-tip events consisting of an unweighted or empty state at the start and seven to eight cumulative weight increments (hexagonal nuts) prior to the tip. The calibration curve for T-BASS no. 1 demonstrates remarkable linearity and reproducibility. The calibration curve for T-BASS no. 2 is slightly non-linear, with a second-order polynomial providing the best fit (R^2 value of 0·997). A linear fit to the T-BASS no. 2 data yields an R^2 of 0·988, in comparison to an R^2 of 0·999 for T-BASS no. 1. Most consistent results for all five traps were obtained with a first-order parameterization that regresses weight against the square-root of the millivolt signal. This model

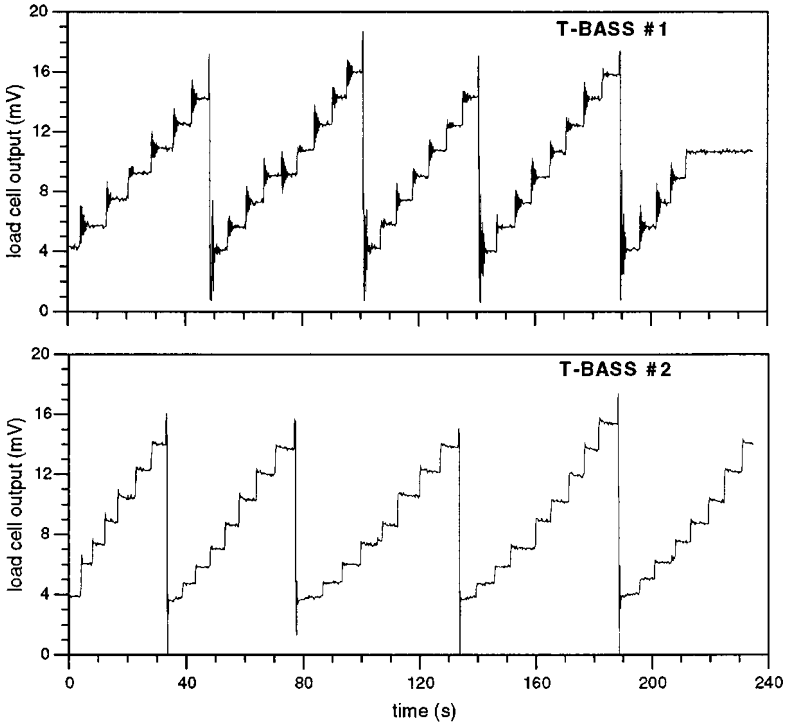

Figure 3. Calibration time series generated by measuring load-cell voltage output (mV) at 5 Hz as calibration weights (hexagonal nuts) are added progressively to the bucket until full capacity is exceeded and tipping (emptying) is induced. Each filling and tipping event corresponds to an entire 'staircase'. The trace for T-BASS no. 1 shows relatively constant voltage steps, indicating linearity of response, whereas T-BASS no. 2 is slightly non-linear. Short-term oscillations in the trace of T-BASS no. 1 are due to the 'jolt' the system receives when a hexagonal nut is tossed into the bucket. Such oscillations are not as apparent in T-BASS no. 2, ostensibly because greater mechanical friction in the bearings damps system response

Table I.

	Voltage (mV)				
	Run 1	Run 2	Run 3	Run 4	Run 5
Weight (g)					
0·00	4·3	4·1	4·2	4·0	4·2
1·13	5·7	5·6	5·8	5·6	5·7
2·26	7·5	7·3	7·5	7·3	7·3
3·39	9·3	9·1	9·0	9·0	8·9
4·52	10·9	10·8	10·8	10·6	10·7
5·65	12·6	12·5	12·5	12·4	end
6·78	14·3	14·3	14·3	14·2	
7·91	tip	16·0	tip	15·8	
Intercept	−2·79	−2·61	−2·78	−2·61	−2·87
Slope	0·670	0·659	0·673	0·666	0·697
R^2	0·999	1·000	0·999	1·000	0·999

Calibration equation using all data in single regression is grams = −2·70 + 0·668 (mV) $R^2 = 0{\cdot}999$

yielded R^2 values in excess of 0·99 for all five assemblies. Nevertheless, some scatter was evident in the calibration data for two of the units and this may be ascribed to inappropriate set-up, inadvertent introduction of sand into the bucket during individual calibration runs by wind, and slight differences in the exact weight of the hexagonal nuts which often had grains of sand sticking to their internal threads. Given the rather crude field conditions during calibration, the overall results are most encouraging.

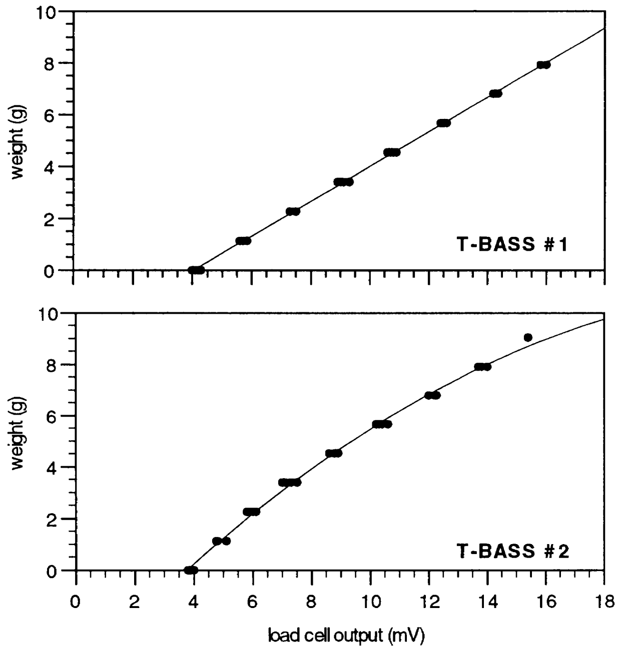

Figure 4. Calibration curves obtained by a least-squares fit to the data gleaned from the time series in Figure 3. R^2 values for these curves are 0·999 and 0·997 for T-BASS no. 1 and T-BASS no. 2, respectively, when all data are used. A straight-line fit to the T-BASS no. 2 data yields an R^2 of 0·988. Note that the regressions were performed with voltage output as the independent variable to yield 'predictive' relationships for later use in converting voltage time series to sediment weight. Values of R^2 do not change when the variables are interchanged

FIELD TEST

Several experiments were conducted in the field during which the T-BASS traps were co-located with instrument masts supporting eight three-cup anemometers (0·10, 0·20, 0·30, 0·50, 0·75, 1·00, 1·25 and 1·75 m) and a wind vane. Figure 5 shows the first hour of a 2 h time series of sediment flux measured by a T-BASS, and a contemporaneous trace of shear velocity derived from the adjacent instrument mast. Data-processing of the T-BASS records involved the following procedure. Each raw-voltage file was examined to identify the tipping events in the digital record. It was found that by subjecting the data to a 3 s moving average, the tipping events could be consistently resolved into three-point sequences that had a characteristic shape. These tipping events were digitally tagged as 'missing values'. At this point, it would be normal to convert voltages to gram weights via an automated computer routine that applies the calibration coefficients obtained earlier. However, these calibration coefficients were thought to be unreliable because a rainstorm occurred directly after the calibration exercise – water and sediment were flushed through the traps and the set-up configuration of the T-BASS components was notably altered. Unfortunately, there was no opportunity to recalibrate the traps prior to the transport event, so the following procedure was utilized. A differencing routine was applied to the voltage time series to yield instantaneous slopes (i.e. the first derivative or rate-of-change of voltage with respect to time) between subsequent data points where the records were continuous (i.e. between 'missing value' tags). The segments corresponding to missing values were then rectified with average slope values determined from local data trends on either side of the tip events. Bucket tips occurred about every 2 min on average, hence the replaced data represent only about 2 per cent of the total record. These reconstituted slope time series were then integrated (summed) to produce a continuous curve of cumulative output voltage rather than the segmented (saw-toothed) traces typical of the raw load-cell output. The cumulative curves were normalized by the maximum, cumulative voltage total for each trap, and converted to gram weight on the basis of total sand

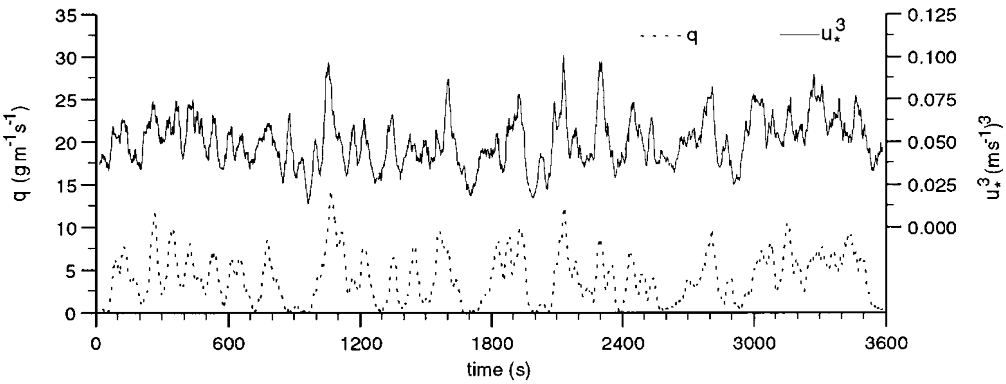

Figure 5. Shear-velocity and sediment-flux time series measured in the field by a T-BASS trap (T50) during a 1h period of sediment transport slightly above the threshold of motion. Data have been smoothed using a 31s moving-average filter

accumulation in the trap reservoir. Actual sediment fluxes were then calculated from these cumulative weight curves by accounting for trap dimensions and running a differencing routine to yield the time-rate-of-change of sediment accumulation; that is, the transport rate in grams per metre of beach width per second. Although we have no independent verification of the actual transport rates in the field, it is promising to note that dividing the total weight of sediment trapped during the 2h run – 502g, in this case – by the number of bucket tips evident in the record (56 tips) yields an average tipping weight for the T-BASS of 9g which was precisely the set-up value.

The shear-velocity trace shown in Figure 5 was processed in a manner similar to the sediment flux data. This was done by first deriving a 1s estimate of u_* from the wind-speed records from all eight anemometers, and then applying a three-point moving average to the 1s u_* estimates. There was considerable short-term variability in the resultant traces, so the data were smoothed a second time using a 31-point moving average in order to highlight the low-frequency fluctuations shown in Figure 5. Note that there is very close correspondence between sediment flux and shear velocity, despite the fact that the flux measurements have not been corrected to take into account shifts in wind direction which affect the efficiency of the trapping shell (Nickling and McKenna Neuman, 1997). This is particularly encouraging since the transport conditions were intermittent, and therefore most susceptible to non-linear response and temporal lag effects.

Figure 6 reveals the type of detailed information evident in a 120s time series of unsmoothed data. Sediment fluxes from three T-BASS traps spaced at 25m intervals along a cross-shore transect parallel to the wind are presented in Figure 6A, whereas Figure 6B shows the contemporaneous shear velocity time series obtained from the instrument tower at the central location (T50). Once again, there is obvious correspondence in the overall trends, with the largest peak in shear velocity (at about 2484s into the run) driving the largest sediment fluxes. A visible lag in measured transport rate is also apparent, with the trap at T25 responding first and the trap at T75 last, separated by time increments of about 2–4s. Moreover, the shear velocity gust at T50 precedes the transport peak at T50 (instrument separation distance of less than 1m in the alongshore) by about 2–4s. Such lag times are in accord with the speculations of Butterfield (1993, p. 312) who suggested that the *primary* response time of mass flux 'may be nearer to two seconds for velocity increments in which U_* just exceeds the threshold condition'. Our field observations are therefore interpreted as being due to a large eddy or wind gust moving through the array and carrying with it a saltation cloud of limited spatial extent. In other portions of the record, the associations between the wind field and transport rate are not as orderly nor as uniform, and the exact nature of these interactions is currently being investigated in further detail as part of a broader research agenda addressing unsteadiness in aeolian sediment transport.

FUTURE DESIGN IMPROVEMENTS

The prototype T-BASS units used in this field study had several minor shortcomings. It is clear that these instruments will not perform ideally under wet conditions (i.e. during rainy or foggy periods) because sand

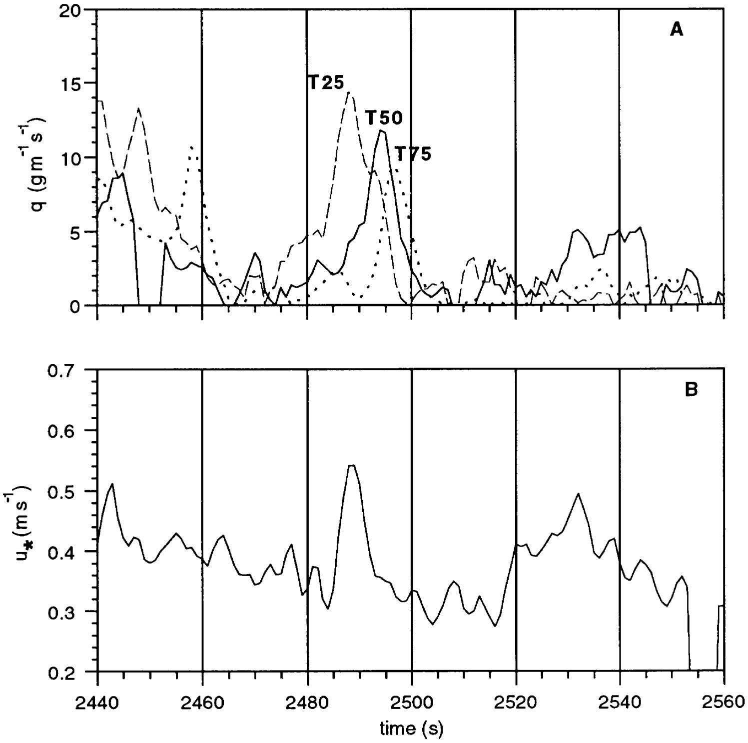

Figure 6. (A) Example of a 120 s period of sediment flux measurements from three T-BASS traps deployed in a cross-shore array at 25 m spacing. The T-BASS trap at T25 (dashed line) was most seaward; T75 (dotted line) was most landward; T50 (solid line) was in an intermediate, central position. (B) The shear velocity trace was obtained by regressing wind speed (measured by eight anemometers on a vertical tower beside T50) against the natural logarithm of elevation at progressive 1 s intervals and then smoothing

tends to stick to all of the trap components, both exterior and interior. This is, of course, a problem with all types of trap (topographic traps excepted). However, it is more bothersome with the prototype T-BASS traps because the tipping-bucket mechanism needs to be accessed and flushed, and this can cause calibration changes due to excess strain on the load cells or to alteration of the mechanical settings. It should be possible to construct a simple, water-resistant cover for the entire trap or to incorporate water-tight seals for the below-ground housing so that moisture and wet sand are prevented from fouling the mechanism during non-measurement periods.

A key design criterion requiring further consideration is reduction of the overall mass of the moving components of the T-BASS relative to the sediment-load capacity of the buckets. Ideally, the accumulating sediment mass should dominate the mechanical system so that component inertia and friction become inconsequential. In practice, this is not possible to achieve. However, the prototype developed in this study was rather massive, and required considerable adjustment to achieve the desired response. It should now be possible to make final decisions about bucket capacities and dimensions, and thereby eliminate many of the adjustable components. In this way, the existing custom-milled, PVC-block design could be replaced by a smaller, lighter and less adjustable unit manufactured to precise tolerances (e.g. injection-moulded), thereby enhancing performance and reducing unit-to-unit variations in response. A smaller, less bulky T-BASS would also decrease the size of the required housing box, which would make it easier to bury and level. More robust, high-performance load cells should be incorporated into the next generation T-BASS – the existing cells were some of the least expensive available and used in the prototype on an experimental basis only. A load cell less susceptible to metal fatigue, with smaller element deflection, higher voltage output gain, and perhaps internally regulated voltage compensation would be desirable. One of the favourable outcomes of this combination of modifications would be virtual elimination of signal spikes and oscillations generated by bucket tips.

Improvements in the string linkage between the pulley and load cell may also lead to enhanced performance of the overall assembly. In particular, the string material should be very light and flexible so as not to place undue strain on the load cell. Yet, it should also be non-elastic and of large tensile strength so that forces are translated to the load cell without modulation. Unfortunately, most string materials stretch or shrink depending on imposed load and environmental conditions (e.g. humidity and temperature), and these may be a source of non-linearity and long-term drift in the calibrations. We are currently testing a new type of non-stretch fishing line that holds promise, as might a Kevlar product or a redesign that eliminates the string linkage altogether.

It may be desirable to increase the overall weight capacity of the tipping buckets. In the original design, there was concern for making the prototype system as sensitive as possible so that even the smallest values of sediment flux could be recorded. The data presented above were collected during periods when the aeolian system was essentially at the threshold-of-motion condition with short gusts of transport separated by lulls of no activity. Even at these relatively small average transport rates, bucket tips were frequent, occurring about every 2 mins. At greater transport rates, the tipping frequency would increase and the resulting transport time series would contain a larger proportion of estimated 'missing value' segments, making interpretation of the data less certain. Increasing the bucket capacity to about 50 g (rather than 10–20 g) would enhance data quality during the intense transport-rate events, presuming that adequate resolution can be retained. This will depend, in large part, on load-cell specifications.

Finally, we would like to draw attention to another continuously weighing aeolian trap reported recently by Jackson (1996). It bears some similarities to ours, and offers some advantages and disadvantages that merit discussion. The trapping system outlined in Jackson (1996) also incorporates a tipping-bucket type mechanism consisting of two cylinders, each with a capacity of 200 g, joined at an angle of 120°. Whereas our bucket assembly was designed to be self-tipping in mechanical fashion, the tipping action in the Jackson (1996) mechanism is initiated electronically by a solenoid. The Jackson (1996) unit offers advantages in ease of set-up because it can be configured to tip at a prescribed load (e.g. 200 g) simply by controlling the solenoid action. However, this comes at the expense of additional electronic componentry needed to link the solenoid to the load-cell output. Our 'passive' units require no control electronics or line power, and our experience shows that the buckets tip at a consistent weight once configured, although the adjustment procedure is more tedious.

Jackson's (1996) bucket–solenoid assembly is mounted directly on a load-cell plate, and does not employ a cantilever system. This simplifies construction and installation but eliminates the possibility of adjustments in instrument resolution and total range. The Jackson (1996) trap was reported to have a resolution of 0·5 per cent FS (i.e. 1g over a range of 200 g) and this is evident from the step-like time series presented by Jackson and McCloskey (1997, Figure 1). The T-BASS units were configured to a much finer resolution of about 0·1g over a range of 10 g, which translates to 1·0 per cent FS (although the actual load cell has a resolution of about 0·25 per cent FS). Note, however, that the cantilever system in the T-BASS allows the full-scale range to be adjusted across approximately an order of magnitude range (i.e. from 2 g to 20 g), and the absolute resolution will change correspondingly (i.e. 0·02 to 0·2 g) because the 1·0 per cent FS specification is fixed. Nominally, then, the T-BASS can be configured to greater sensitivity. Given that sediment fluxes encountered during field experiments may range across several orders of magnitude, the cantilever approach appears to offer a significant advantage in that it can be adjusted according to transport intensity. In practice, this comes at the expense of additional set-up time, and we note that such time may not be available in cases of rapidly changing field conditions. Ideally, an aeolian trapping device would have a resolution approaching 0·001 per cent FS across a large total-load range so that adjustments are not needed. Unfortunately, this is well beyond the ability of most inexpensive load cells, which have typical resolutions around 0·1 per cent FS, at best.

Perhaps the most significant difference between the approach of Jackson (1996) and that reported here lies in the geometry and orientation of the trapping orifice. Jackson (1996) employs a circular orifice mounted horizontally and flush with the sediment bed. Ours incorporates the more traditional, vertically mounted wedge shell with an inlet duct and slit orifice. These represent fundamentally different approaches to the trapping problem predicated on specific assumptions about the nature of aeolian saltation that are incommensurable. Detailed consideration of the relative merits of vertical versus horizontal trap styles is beyond the scope of the present paper, but we note in passing that both systems could be easily modified to operate in either mode by adding or removing a vertical shell. Nevertheless, there are implications for the resolving ability of the

weighing mechanism because the size of the trap opening dictates the trapping rate for any given sediment flux. For a large-diameter horizontal trap, the trapping rate is expected to be large (even for relatively small sediment fluxes) and therefore a sensitive weighing mechanism may not be necessary. We presume that this is why Jackson (1996) opted to incorporate a 200 g bucket size. For a vertical trap, however, the width of the slit orifice is critical to the efficiency of the trap because the geometry of the wedge affects the aerodynamic character of flow around the trap. Narrow slit widths are preferable, and therefore the trapping rate is expected to be small (even during intense transport periods) and a sensitive weighing mechanism becomes essential.

SUMMARY

A continuously weighing tipping-bucket assembly was designed and incorporated into an aeolian sediment trap, and several of these units were field tested with encouraging results. Field-based calibrations show their response to be near-linear with R^2 values for the regressions in excess of 0·99 for all cases. Two-hour-long data sets collected during a transport event near the threshold-of-motion condition are revealing of several interesting relationships (such as the nature of the temporally lagged association between the wind field and the sediment flux), and these data demonstrate the future potential of the tipping-bucket assembly. It offers the advantage of precise high-frequency measurement of aeolian sediment flux for the full duration of wind events, without the need to halt measurements and empty traps during the event. Such data are invaluable to refining our understanding of the mechanics of aeolian transport and to investigating the variability inherent to natural systems.

ACKNOWLEDGEMENTS

Thanks are extended to Victor and Ramone (USC Academic Workshops) for their patience and skill in translating our rough sketches and ideas into a working prototype, to Drs Davidson-Arnott and Nickling (University of Guelph) for commenting on earlier drafts of the manuscript, and to the Geography and Regional Science Program (National Science Foundation) for providing financial support (Grant Numbers: SES-9158230; SES-9511529). Additional technical details on T-BASS design and construction may be obtained by contacting the authors.

REFERENCES

Anderson, R. A., Sorensen, M. and Willetts, B. B. 1991 ‘A review of recent progress in our understanding of aeolian sediment transport’, *Acta Mechanica*, Supp. **1**, 1–19.

Arens, S. M. 1994. *Aeolian processes in the Dutch foredunes*. PhD Thesis, Department of Physical Geography and Soil Science, Universiy of Amsterdam, 150 pp.

Arens, S. M. 1996. ‘Rates of aeolian transport on a beach in a temperate humid climate’, *Geomorphology*, **17**(1–3), 3–18.

Bagnold, R. A. 1936. ‘The movement of desert sand’ *Proceedings of the Royal Society of London, Series A*, **157**, 594–620.

Bagnold, R. A. 1941. *The Physics of Blown Sand and Desert Dunes*, William Morrow, New York, 265 pp.

Bauer, B. O., Davidson-Arnott, R. G. D., Nordstrom, K. F., Ollerhead, J. and Jackson, N. L. 1996. ‘Indeterminacy in aeolian sediment transport across beaches’, *Journal of Coastal Research*, **12**(3), 641–653.

Butterfield, G. R. 1991. ‘Grain transport rates in steady and unsteady turbulent air flows’, *Acta Mechanica*, Supp. **1**, 97–122.

Butterfield, G. R. 1993. ‘Sand transport response to fluctuating wind velocity’, in Clifford, N. J., French, J. R. and Hardisty, J. (Eds), *Turbulence: Perspectives on Flow and Sediment Transport*, John Wiley, New York, 305–335.

Davidson-Arnott, R. G. D. and Law, M. N. 1996. ‘Measurement and prediction of long-term sediment supply to coastal foredunes’ *Journal of Coastal Research*, **12**(3), 654–663.

Dijk, P. M. van and Hollemans, W. A. 1991. *Wind erosion measurements on the island of Schiermonnikoog Report III, The calibration of wind erosion measuring devices by means of wind tunnel research*, Wageningen Agricultural University, Department of Irrigation and Soil and Water Conservation, 38 pp.

Fryberger, S. G., Ahlbrandt, T. A. and Andrews, S. 1979. ‘Origin, sedimentary features, and significance of low-angle eolian sand sheet deposits, Great Sand Dunes National Monument and vicinity, Colorado’, *Journal of Sedimentary Petrology*, **49**, 733–746.

Fryberger, S. G., Al-Sari, A. M., Clisham, Th. J., Rizvi, S. A. R. and Al-Hinai, K. G. 1984. ‘Wind sedimentation in the Jafurah sand sea, Saudi Arabia’, *Sedimentology*, **31**, 413–431.

Gares, P. A., Davidson-Arnott, R. G. D., Bauer, B. O., Sherman, D. J., Carter, R. W. G., Jackson, D. W. T. and Nordstrom, K. F. 1996. ‘Alongshore variations in aeolian sediment transport: Carrick Finn Strand, Ireland’, *Journal of Coastal Research*, **12**(3), 673–682.

Goldsmith, V., Rosen, P. and Gertner, Y. 1990. ‘Eolian transport measurements and comparison with theoretical transport in Israeli coastal dunes’ in Nordstrom, K. F., Psuty, N. P. and Carter, R. W. G. (Eds), *Coastal Dunes: Process and Morphology*, John Wiley, New York, 77–101.

Greeley, R., Blumberg, D. G. and Williams, S. H. 1996. 'Field measurements of the flux and speed of windblown sand', *Sedimentology*, **43**, 41–52.

Horikawa, K., Hotta, S., Kubota, S. and Katori, S. 1984. 'Field measurement of blown sand transport rate by trench trap', *Coastal Engineering in Japan*, **27**, 213–232.

Jackson, D. W. T. 1996. 'A new, instantaneous aeolian sand trap design for field use', *Sedimentology*, **43**, 791–796.

Jackson, D. W. T. and McCloskey, J. 1997. 'Preliminary results from a field investigation of aeolian sand transport using high resolution wind and transport measurements', *Geophysical Research Letters*, **24**(2), 163–166.

Kroon, A. and Hoekstra, P., 1990. 'Eolian sediment transport on a natural beach' *Journal of Coastal Research*, **6**, 367–379.

Leatherman, S. P. 1978. 'A new eolian sand trap design', *Sedimentology*, **25**, 303–306.

Lee, J. A. 1984. *Sand transport on a barchan dune*, MA thesis, Geography Department, University of California, Los Angeles.

Lee, J. A. 1987. 'A field experiment on the role of small scale wind gustiness in aeolian transport', *Earth Surface Processes and Landforms*, **12**, 331–335.

Nickling, W. G. and McKenna Neuman, C. 1997. 'Wind tunnel evaluation of a wedge-shaped aeolian sediment trap', *Geomorphology*, **18**, 333–345.

Nordstrom, K. F., Bauer, B. O., Davidson-Arnott, R. G. D., Gares, P. A., Carter, R. W. G., Jackson, D. W. T. and Sherman, D. J. 1996. 'Offshore aeolian transport across a beach: Carrick Finn Strand, Ireland', *Journal of Coastal Research*, **12**(3), 664–672.

Shao, Y., McTainsh, G. H., Leys, J. F. and Raupach, M. R. 1993. 'Efficiencies of sediment samplers for wind erosion measurement' *Australian Journal of Soil Research*, **31**, 519–532.

Sherman, D. J. 1990. 'A method for measuring aeolian sediment transport rate' in Davidson-Arnott, R. W. G. (Ed.), *Proceedings of the Symposium on Coastal Sand Dunes*, National Research Council of Canada, Ottawa, 37–47.

Spaan, W. P. and van den Abeele, G. D. 1991. 'Wind borne particle measurements with acoustic sensors', *Soil Technology*, **4**, 51–63.

